

## NEARLY TIME-OPTIMAL PATHS FOR A GROUND VEHICLE

David A. Anisi \* Johan Hamberg \*\* Xiaoming Hu \*

\* *Optimization and Systems Theory*  
*Royal Institute of Technology*  
*SE-10044 Stockholm, Sweden.*

\*\* *Department of Autonomous Systems*  
*Swedish Defence Research Agency*  
*SE-172 90 Stockholm, Sweden.*

**Abstract:** It is well known that the sufficient family of time-optimal paths for both Dubins' as well as Reeds-Shepp's car models consist of the concatenation of circular arcs with maximum curvature and straight line segments, all tangentially connected. These time-optimal solutions suffer from some drawbacks. Their discontinuous curvature profile, together with the wear and impairment on the control equipment that the bang-bang solutions induce, calls for "smoother" and more supple reference paths to follow. Avoiding the bang-bang solutions also enhances the robustness with respect to any possible uncertainties.

In this paper, our main tool for generating these nearly time-optimal, but nevertheless continuous-curvature paths, is to use the Pontryagin Maximum Principle (PMP) and make an appropriate choice of the Lagrangian function. Despite some rewarding simulation results, this concept turns out to be numerically divergent at some instances. Upon a more careful investigation, it can be concluded that the problem at hand is nearly singular. This is seen by applying the PMP to Dubins' car and studying the corresponding two point boundary value problem, which turn out to be singular. This is thus a counterexample to the widespread belief that all the information about the motion of a mobile platform lies in the initial values of the auxiliary variables associated with the PMP.

**Keywords:** Motion Planning, Optimal Control, Pontryagin Maximum Principle, UGV

### 1. INTRODUCTION

In his pioneering work (Dubins, 1957), L.E. Dubins considered a problem which later was interpreted as finding the shortest continuously differentiable path between two given points taken by a car, for which the starting and ending directions are specified. In addition, the car is required to move with unit speed and subject to a minimum turning radius constraint. The car model considered, is the unicycle robot model

$$\begin{aligned}\dot{x} &= v \cos \varphi \\ \dot{y} &= v \sin \varphi \\ \dot{\varphi} &= \omega,\end{aligned}\tag{1}$$

where the reference point  $(x, y) \in \mathbb{R}^2$  is taken as the midpoint of the car's rear axle,  $\varphi$  denotes the car's orientation angle, while  $v$  and  $\omega$  denote the linear and lateral control inputs respectively. Model (1) implies that the car model is subject to a nonholonomic constraint

$$\dot{x} \sin \varphi - \dot{y} \cos \varphi = 0.$$

In the same paper, Dubins showed that every time-optimal path interconnecting any two given points in the state space, is the concatenation of circular arcs with maximum curvature and straight line segments, all tangentially connected. This basic path segments' duration and mutual order however is a more delicate matter.

In 1990, J.A. Reeds and L.A. Shepp extended these

results to the case when the car is augmented with a reverse gear (Reeds and Shepp, 1990). Although appearing insignificant, allowing the car to perform backwards motions as well, turns out to have implications on various issues, including the car's controllability and symmetry properties (Sussman and Tang, 1991). The time-optimal paths will however still be of the same type as those associated with Dubins' car, i.e. essentially bang-bang solutions.

The above mentioned bang-bang solutions, suffer from some drawbacks. Their discontinuous curvature profile, together with the wear and impairment on the control equipment that the bang-bang solutions induce, calls for "smoother" and more supple reference paths to follow. Stated more precisely, we would like the generated paths to have continuous and bounded curvature (i.e.  $\in C^2$ ). Important contributions to the study of this problem have been given by Boissonnat *et. al* in (Boissonnat *et al.*, 1994), where they proved that all candidates for optimality are made of the concatenation of circular arcs, straight line segments and clothoid pieces. Unfortunately it turns out that the optimal paths consist of infinity many pieces whenever they contain a straight line segment, which clearly occurs whenever the configurations to be connected are far apart. Avoiding this, Sheuer and Laugier have considered the solution when the number of switchings are restricted to a finite number (Scheuer and Laugier, 1998).

Our approach is to investigate how tools from Optimal Control and above all the Pontryagin Maximum Principle (PMP) can be used for generating such nearly time-optimal paths. We thus consider the following Optimal Control Problem:

$$\begin{aligned} & \text{minimize } \int_0^T \mathcal{L}(x, v, \omega) dt \\ & \text{subject to} \\ & \dot{x}(t) = [v(t) \cos \varphi(t), v(t) \sin \varphi(t), \omega(t)]^T \\ & x(0) = X_i \quad x(T) = X_f \\ & v(\cdot) \in [-1, 1] \quad \omega(\cdot) \in [-1, 1] \\ & x(\cdot) \in \mathcal{X} = \mathbb{R}^2 \times S^1 \\ & \mathcal{L}(x, v, \omega) : \mathcal{X} \times \mathbb{R}^2 \rightarrow \mathbb{R} \end{aligned}$$

The choice of an appropriate Lagrangian function,  $\mathcal{L}$ , should clearly be made with some practical, control-motivated reasons in mind. What objectives to consider when making that choice and examples of suitable Lagrangian functions are presented in section 2. Some of the advantages of generating nearly time-optimal paths are illustrated in section 3 where some simulation results are presented. It turns out however, that the presented concept suffers from numerical instability properties. The origin of this undesirable behavior is revealed in section 4. Finally, the conclusions and a brief summary can be found in section 5.

## 2. SELECTION OF THE LAGRANGIAN

In this section we discuss how to make a good choice for an arbitrary Lagrangian function,  $\mathcal{L}$ , with some practical, control-motivated reasons in mind. We have three main objectives that should be reflected in the Lagrangian: Firstly, we have the obvious intention of reaching the terminal configuration as fast as possible. This target is reached by including an *integral constant*,  $\mathcal{L}_1 = 1$  in the integral cost function,  $\mathcal{L}$ .

Secondly, avoiding the drawbacks of time-optimal solutions, involves introducing a *penalty* for steering the car with control values close to their boundary points. The penalty function enables us to encourage a more moderate driving style. Finally, technological limitations, such as the car's turning radius, normally leave us with a restricted control domain. Our third and last objective when selecting  $\mathcal{L}$ , is to handle input saturations in a convenient manner. A direct approach, involves adopting an integral cost function, having the form of a well. For instance

$$\mathcal{L}_3 = \begin{cases} 0 & \text{if } u \in [-1, 1] \\ \infty & \text{else} \end{cases}$$

provides a solid *barrier*, in which the control function is allowed to take its values (here  $u$  refers to either of the two control inputs indistinctly). However, as illustrated in the up-following discussion, by making a more clever selection of  $\mathcal{L}$ , we show a more subtle and implicit way to handle input restrictions.

Let us, instead of simply bonding the contribution of our three objectives together by setting  $\mathcal{L} = \sum_{i=1}^3 \mathcal{L}_i$ , use superposition to weld the penalizing properties of  $\mathcal{L}_2$  with the off-barriering characteristics of  $\mathcal{L}_3$  and express them by means of a common cost function,  $\mathcal{L}_0$ . In order to obtain even more versatility, let  $\mathcal{L}_0$  be proportional to what we call a *design parameter*,  $\varepsilon$ . Then by adjusting  $\varepsilon$ , we will be able to decide how close to the time-optimal solution we wish to find ourselves. Setting  $\varepsilon = 0$  yields  $\mathcal{L} = \mathcal{L}_1 = 1$  and thus equals this with the time-optimal problems considered in (Dubins, 1957) and (Reeds and Shepp, 1990). Then by gradually tuning  $\varepsilon$  up, we penalize the usage of the boundary points of the control domain increasingly, and hence put more value into a moderate driving style. This of course occurs at the expense of time-optimality.

We study the construction of nearly time optimal paths by starting with the following intuitively justified candidate for an appropriate Lagrangian function,

$$\mathcal{L} = \mathcal{L}_0 + \mathcal{L}_1 = \frac{\varepsilon}{2(1-u^2)} + 1, \quad (2)$$

which certainly possesses both the desired penalizing and restricting properties. In this case, the Hamiltonian becomes

$$\begin{aligned} \mathcal{H} &= \lambda_x v \cos \varphi + \lambda_y v \sin \varphi + \lambda_\varphi \omega \\ &\quad - \frac{\varepsilon}{2(1-v^2)} - \frac{\varepsilon}{2(1-\omega^2)} - 1. \end{aligned}$$

Maximizing this Hamiltonian point-wise, involves finding the roots of its partial derivatives

$$\frac{\partial \mathcal{H}}{\partial v} = \sigma - \frac{\varepsilon v}{(1-v^2)^2} = 0 \quad (3)$$

$$\frac{\partial \mathcal{H}}{\partial \omega} = \lambda_\varphi - \frac{\varepsilon \omega}{(1-\omega^2)^2} = 0, \quad (4)$$

where  $\sigma = \lambda_x \cos \varphi + \lambda_y \sin \varphi$ . By virtue of the similarities between equations (3) and (4), it suffices to study either one. Consider then the latter and initially assume  $\lambda_\varphi \neq 0$  (the  $\lambda_\varphi \equiv 0$  case, will be examined later). Then, we are able to write equation (4) as

$$\Delta(\omega) := (1 - \omega^2)^2 - \frac{\varepsilon}{\lambda_\varphi} \omega = 0. \quad (5)$$

Apparently, (5) would only have real roots on the  $\text{sign}(\lambda_\varphi)\omega \geq 0$  half axis. Since  $\Delta(0) > 0$ ,  $\Delta(\text{sign}(\lambda_\varphi)1) < 0$ , and  $\text{sign}(\lambda_\varphi)\Delta'(\omega) < 0$  for all  $\text{sign}(\lambda_\varphi)\omega \in (0, 1)$ , we conclude that only one root lies in the admissible interval, or equivalently that the point-wise maximization of the Hamiltonian has a unique solution. In figure 1, the real roots of equation (5) are plotted as the intersection points of the functions  $f_1(\omega) = (1 - \omega^2)^2$  and  $f_2(\omega) = \frac{\varepsilon}{\lambda_\varphi} \omega$ .

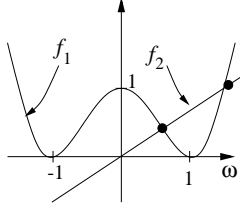


Fig. 1. The roots of equation (5) correspond to the intersection points of  $f_1(\omega) = (1 - \omega^2)^2$  and  $f_2(\omega) = \frac{\varepsilon}{\lambda_\varphi} \omega$ .

In the time-optimal case ( $\varepsilon = 0$ ), the slope of  $f_2(\omega)$  is zero, hence the two possible values for  $\omega^*$  are  $\pm 1$ . This naturally corresponds to the minimum radius left- and right turn respectively. This holds for all non-zero values on  $\lambda_\varphi$ . But as we set  $\varepsilon \neq 0$ ,  $\text{sign}(\lambda_\varphi)$  only determines the quadrant of location of the root. Its exact value is indefinite but nevertheless, continuously varying with  $\lambda_\varphi$ . We further note that the boundary values of the lateral control, are not reached unless  $\lambda_\varphi \rightarrow \infty$ , excluding the occurrence of bang-bang solutions. These are very desirable properties.

Further, since  $\lambda_\varphi = 0$ ,  $\omega = 0$ , is a solution to equation (4), and we have shown that only one root lies in the admissible interval when  $\lambda_\varphi \neq 0$ , one can easily use the implicit function theorem to show that  $\omega^*$  varies continuously as  $\lambda_\varphi$  evolves and changes sign.

Although it is fully possible to analytically solve equation (4) for  $\omega^*$ , the resulting expressions looks anything but tidy. Therefore, we approximate  $f_1(\omega)$ ,  $\omega \in [-1, 1]$  in figure 1, with the upper half of a unit circle. With this approach, expressing the lateral control as a function of  $\varepsilon$ , reduces to finding the point of intersect

between a straight line and a semi-circle. Referring to figure 2 and considering the fact that  $\tan \vartheta$ , equals the direction of the straight line  $\frac{\varepsilon}{\lambda_\varphi}$ , we get

$$\omega^* = \cos \vartheta = \frac{1}{\sqrt{\tan^2 \vartheta + 1}} = \frac{\lambda_\varphi}{\sqrt{\varepsilon^2 + \lambda_\varphi^2}}. \quad (6)$$

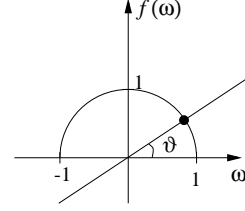


Fig. 2. The circle segment approximates  $f_1(\omega)$ ,  $\omega \in [-1, 1]$  in figure 1 and leads to some rewarding results.

We observe that by setting  $\varepsilon = 0$  in equation (6), we get  $\omega^* = \text{sign}(\lambda_\varphi)$ , which is to be recognized as the optimal control associated with the time-optimal case. Then by gradually tuning up the design parameter, we damp the fluctuating behavior of the optimal control whenever  $\lambda_\varphi$  changes sign, and thereby replace the bang-bang solutions with smoother and more pliable paths (cf. figure 3).

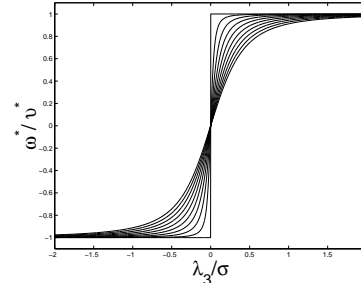


Fig. 3. The  $\varepsilon$ -dependence of the optimal control. Here,  $\varepsilon$  varies between 0 and 0.5.

Analogous reasoning applies for the linear control  $v^*$ , with  $\sigma$  playing the role of  $\lambda_\varphi$ . The summarizing results of this example will therefore be

$$\boxed{\begin{aligned} v^* &= \frac{\sigma}{\sqrt{\varepsilon^2 + \sigma^2}} \\ \omega^* &= \frac{\lambda_\varphi}{\sqrt{\varepsilon^2 + \lambda_\varphi^2}} \end{aligned}} \quad (7)$$

#### Nearly time-optimal paths

Motivated by the perspicuous results and their desirable properties obtained in the solution to the optimal control problem defined by (2), we make the following choice for Lagrangian

$$\mathcal{L} = 1 - \varepsilon \sqrt{1 - u^2}, \quad (8)$$

its circular form, evidently influenced by the approximation made in the previous example. The Hamiltonian then becomes

$$\mathcal{H} = \lambda_x v \cos \varphi + \lambda_y v \sin \varphi + \lambda_\varphi \omega + \varepsilon \sqrt{1-v^2} + \varepsilon \sqrt{1-\omega^2} - 1 \quad (9)$$

and its point-wise maximization gives

$$\begin{aligned} \frac{\partial \mathcal{H}}{\partial v} = \sigma - \frac{\varepsilon v}{\sqrt{1-v^2}} = 0 &\Rightarrow \sqrt{1-v^2} = \frac{\varepsilon}{\sigma} v \\ \frac{\partial \mathcal{H}}{\partial \omega} = \lambda_\varphi - \frac{\varepsilon \omega}{\sqrt{1-\omega^2}} = 0 &\Rightarrow \sqrt{1-\omega^2} = \frac{\varepsilon}{\lambda_\varphi} \omega, \end{aligned}$$

where  $\sigma = \lambda_x \cos \varphi + \lambda_y \sin \varphi$ . In accordance with previous calculations, the expressions for optimal control will coincide with those presented in (7).

Reflecting upon what this choice of the Lagrangian has resulted in, we are able to pinpoint some distinguished characteristics; firstly, notice that  $\mathcal{L}_0$  in this case, conceptually differs from the ones considered so far. This one merely satisfies our penalizing objective, while no solid control restricting barrier, is imposed. Nevertheless, we can conclude from the expressions for the optimal control (7), that even this requirement is met. This provides us with a more subtle and implicit approach for handling control constraints. Secondly, we observe that we have the possibility to make a continuous and arbitrary adjustment of the design parameter, in order to damp the fluctuating behavior of the optimal control pertaining to time-optimal solutions. This introduced flexibility, is illustrated in figure 3 and enables us to designedly avoid time-optimal solutions and their before-mentioned drawbacks. There is yet another advantage, which is to be discussed more thoroughly in section 4, and that is the smoothing effect of the optimal control on the systems Hamiltonian function.

### 3. SIMULATIONS AND EXPERIMENTS

In addition to the systems dynamics that governs the time evolution of the state vector and the optimal control law specified by equation (7), the time evolution of the auxiliary variables will be of interest when we carry out our simulations. The *Two Point Boundary Value Problem* that we ought to consider is

$$\begin{cases} \dot{x} = v^* \cos \varphi \\ \dot{y} = v^* \sin \varphi \\ \dot{\varphi} = \omega^* \\ \dot{\lambda}_x = 0 \\ \dot{\lambda}_y = 0 \\ \dot{\lambda}_\varphi = v^* [\lambda_y \cos \varphi - \lambda_x \sin \varphi] \end{cases} \quad \text{s.t. } x(0) = X_i \text{ and } x(T) = X_f, \quad (10)$$

where  $v^*$  and  $\omega^*$  are chosen in accordance with (7).

Figure 4 is the outcome of our first simulation where the objective is to steer the car between  $X_i = [-2, 2, -\frac{\pi}{2}]$  and  $X_f = [0, 0, -\frac{\pi}{2}]$ . The time-optimal path is obtained by setting  $\varepsilon = 0$  and is sketched with a

thicker line in figure 4. However, by tuning  $\varepsilon$  up gradually, we are able to digress from this time-optimal (bang-bang) solution in a continuous and controlled manner.

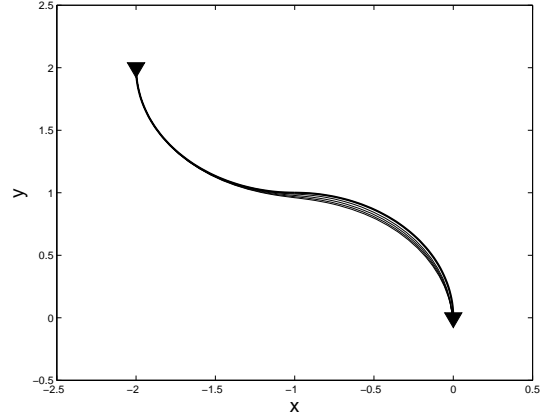


Fig. 4. By tuning  $\varepsilon$  up gradually, we digress from the time-optimal (bang-bang) solution.

The embedded robustness in these more supple paths, is illustrated in our next simulation where we study the flexibility of the mobile platform with respect to changes in a *prescribed* time of arrival,  $\hat{T}$ . Such flexibility is of great importance when simultaneous rendezvous problems for a team of platforms are considered. Referring to figure 5 and 6, the task in all five trials is to steer between the same two prescribed configurations. However, the prescribed time of arrival,  $\hat{T}$ , varies. As seen in figure 5, when  $\hat{T}$  is set to 2, the linear velocity  $v^*(t)$ , almost takes its highest value, i.e. equals 1, during the entire time interval - this in order to be able to make it to the final configuration at the prescribed time of arrival. But as we set  $\hat{T}$  to higher and higher values, we note how the linear velocity decreases and a more moderate driving style is being adopted.

The corresponding control in the lateral direction  $\omega^*(t)$ , can be seen in figure 6, where we note that for  $\hat{T} = 2$ ,  $\omega^*(t)$  is relatively bang-bang. But as the value of the arrival time increases, the fluctuating behavior of the angular velocity is being damp, resulting in much smoother paths.

These two above-mentioned simulations, illustrate that the proposed control law meets all our requirements and fulfills all our objectives thus far. However, the numerical computations in the shooting method, turns out to be divergent at some instances. In the next section, we are to locate the origin of this undesirable behavior.

### 4. THE SINGULAR PROPERTY OF THE PROBLEM

In order to get a glimpse beneath the surface and gain some insight about the reasons for the shooting method to diverge, we recur to Dubins' problem. The

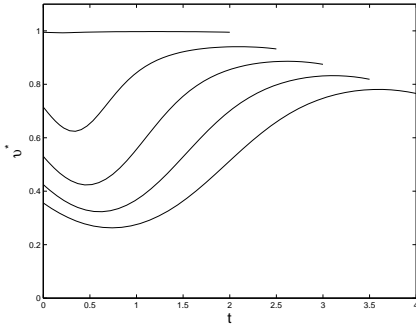


Fig. 5. As the time of arrival sets to higher values, a more moderate driving style is being adopted. By decreasing the value of the linear velocity, the car “wastes time” and is thereby able to adjust its time of arrival within a considerable interval of time.

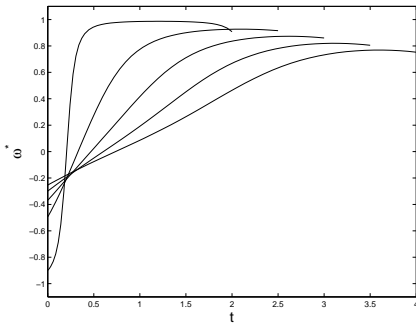


Fig. 6. As the time of arrival is postponed, the generated paths become smoother.

Hamiltonian function in this case becomes (cf. (Anisi, 2003))

$$H(x, \lambda) = \lambda_x \cos \varphi + \lambda_y \sin \varphi + |\lambda_\varphi| - 1. \quad (11)$$

Since neither of the state variables specifying the position of the platform (i.e.  $x$  or  $y$ ) are included in  $H$ , the corresponding auxiliary variables,  $\lambda_x$  and  $\lambda_y$ , are cyclic, that is they are time constants. Then by setting

$$\begin{cases} \lambda_x = -\mu \cos \varphi_0 \\ \lambda_y = \mu \sin \varphi_0, \end{cases}$$

we are able to write equation (11) as

$$H = \mu \cos(\varphi - \varphi_0) + |\lambda_\varphi| - 1.$$

Now, from the standard results regarding the PMP, it follows that the Hamiltonian is constant on a full trajectory - that is, the level curves of  $H$  correspond to different trajectories for the mobile platform. Let us therefore pay attention to these. The level curves of the system are sketched by means of *Mathematica* in figure 7. The reason for rewriting the cyclic auxiliary variables ( $\lambda_x$  and  $\lambda_y$ ) in terms of  $\mu$  and  $\varphi_0$  might be more obvious now, since the constant  $\varphi_0$  solely adjusts the horizontal alignment of the level curves, while the constant  $\mu$  specifies their depth. We are thus able to study the full motion of the mobile platform by just paying attention to the time evolution of two variables, namely  $\varphi(t)$  and  $\lambda_\varphi(t)$ . Generating a typical path for Dubins' car which consists of a circular movement,

followed by a straight line movement followed by yet another movement on a circular arc, is a singular problem and can not be achieved by just finding an appropriate value on  $\lambda_\varphi(0)$ . Notice that  $\lambda_v(0)$  and  $\lambda_\omega(0)$  do not effect the shape of the level curves.

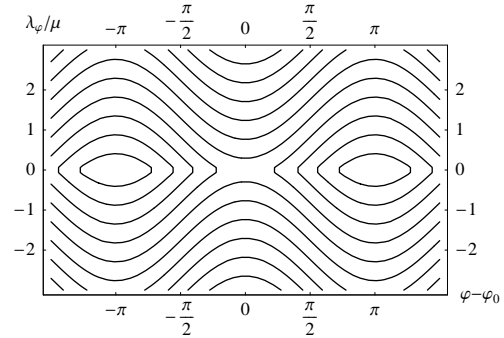


Fig. 7. The level curves of the Hamiltonian correspond to different trajectories of the mobile platform. Generating a path for Dubins' car by choosing an appropriate  $\lambda(0)$  is a singular problem.

Same conclusion can be drawn from studying figure 8 where the level surface of the Hamiltonian can be seen. We note that two smooth surfaces are seamed together at a joint, centered at the axis along  $\lambda_\varphi = 0$ . Hence the Hamiltonian has different derivatives on different sides of this joint, making the right hand side of the TPBVP (10) a discontinuous function. Then it follows from standard results on differential equations, that in the case of a discontinuous dynamics, not even existence of a solution is guaranteed, even less its optimality or uniqueness. It is a widespread idea that all the information about the motion of a mobile platform lies in the initial values of the auxiliary variables  $\lambda(0)$ . We have however shown that this does not hold true in all cases and that a more careful analysis of the system properties must be carried out in order to be able to draw any conclusions about that matter.

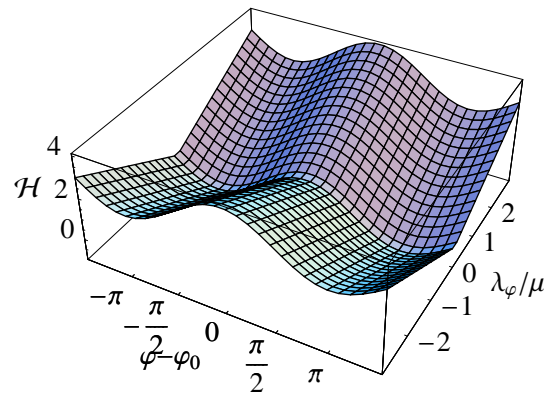


Fig. 8. The level surface of the Hamiltonian function for Dubins' problem.

Let our next study involve the Hamiltonian when we utilize the control law specified by equation (7).

Combining this with equation (9) yields the following expression for the Hamiltonian function

$$H_{\text{CRS}}(x, \lambda) = \sqrt{\varepsilon^2 + \sigma^2} + \sqrt{\varepsilon^2 + \lambda_\varphi^2} - 1. \quad (12)$$

To fully understand the advantage with (12), let us present the expression for the Hamiltonian for the Reeds-Shepp car and make a comparison (cf. (Anisi, 2003)).

$$H_{\text{RS}}(x, \lambda) = |\sigma| + |\lambda_\varphi| - 1$$

Comparing this with equation (12), we see that by introducing  $\varepsilon$ , we have abolished the discontinuous properties of  $H_{\text{RS}}$ .  $H_{\text{CRS}} \in \mathcal{C}^1$  and do not have a sharp joint. Possessing a continuously differentiable Hamiltonian is noticeable, since it improves and rectifies the numerical issues of the optimal control problem. However, our ambition is to produce *nearly time-optimal* paths, hence we are concerned with rather small values on the design parameter  $\varepsilon$ . As a result, the corresponding improvements in the numerical properties of the problem at hand, will be comparatively small. In order to get a significant improvement and obtain numerically stable algorithms for real-life applications, we have to tune  $\varepsilon$  up to considerable values. That in turn, penalizes the input signals accordingly and results in paths that differ too much from the time-optimal paths to be classified as “nearly time-optimal”.

We have also investigated the possible approach of choosing  $\mathcal{L}$  differently, so that better numerical properties are obtained for relatively low values on  $\varepsilon$ . A representative candidate for such a choice is  $\mathcal{L} = \varepsilon \ln(1-u^2) + 1$ . The common characteristic of suitable Lagrangians for this approach, is that they put a considerable penalty on the input signal even for relatively low values on  $\varepsilon$ . The net outcome of the simulations adopting such Lagrangian is however similar to the ones aforementioned. The bottom line is that there is obviously a trade-off between the numerical stability of the problem and the magnitude of the penalty imposed on the control function on one hand, and yet another one between the imposed penalty and the appearance of the generated paths.

## 5. SUMMARY AND DISCUSSION

In this paper, we investigate how tools from Optimal Control and above all the Pontryagin Maximum Principle (PMP) can be used to generate nearly time-optimal, but nevertheless continuous-curvature paths for a ground vehicle. The unicycle robot model have been used to describe the kinematics of the vehicle. Initially, we discussed what objectives to consider when making the choice for an arbitrary Lagrangian function and exemplified some appropriate choices that satisfies all our objectives. These qualities were then confirmed by the presented simulation results. The numerical computations in the shooting method however, turn out to be divergent at some instances. Upon a more careful investigation, we could conclude

that the problem at hand is nearly singular.

It is possible to rectify the numerical difficulties to some extent by either significantly increasing the value of the design parameter  $\varepsilon$ , or choosing another type of Lagrangian. The common characteristic of suitable Lagrangians for this line of action, is that they put a considerable penalty on the input signal even for relatively low values on  $\varepsilon$ . There is obviously a trade-off between the numerical stability of the problem and the magnitude of the penalty imposed on the control function on one hand, and yet another one between the imposed penalty and the appearance of the generated paths. Hence, the generated paths when striving to get a numerically stable algorithm for real-life applications, are too unlike the time-optimal bang-bang solutions, to be classified as “nearly time-optimal” paths and thus have to be disregarded.

When striving to localizing the origin of the above mentioned undesirable behavior, we concluded that adopting shooting method on Dubins’ problem is a singular problem. It is a widespread belief that all the information about the motion of a mobile platform lies in the initial values of the auxiliary variables associated with the PMP. We have however shown that this does not hold true in all cases and that a more careful analysis of the system properties must be carried out in order to be able to draw any conclusions about that matter.

## 6. REFERENCES

- Anisi, David A. (2003). “Optimal Motion Control of a Ground Vehicle”. Master’s thesis. Royal Institute of Technology (KTH), Stockholm, Sweden.
- Boissonnat, J.D., A. Cerezo and J. Leblond (1994). “A note on shortest paths in the plane subject to a constraint on the derivative of the curvature”. Research report 2160. Inst. Nat. de Recherche en Informatique et en Automatique.
- Dubins, L.E. (1957). “On curves of minimal length with a constraint on average curvature, and with prescribed initial and terminal positions and tangents”. *American Journal of Mathematics* **79**, 497–516.
- Reeds, J.A. and L.A. Shepp (1990). “Optimal paths for a car that goes both forwards and backwards”. *Pacific Journal of Mathematics* **145**(2), 367–393.
- Scheuer, A. and Ch. Laugier (1998). “Planning Sub-Optimal and Continuous-Curvature Paths for Car-Like Robots”. In: *IEEE/RSJ International Conference on Intelligent Robots and Systems*. Vol. 1. pp. 25–31.
- Sussman, Hector J. and Guoqing Tang (1991). “Shortest paths for the Reeds-Shepp car: a worked out example of the use of geometric techniques in nonlinear optimal control”. Technical Report SYCON-91-10. Department of Mathematics, Rutgers University.

hur ser detta ut ? (?)